Desalination and Water Treatment
www.deswater.com

doi: 10.5004/dwt.2018.22195

113 (2018) 296–306
May

Optimized synthesis of polyacrylamide (PAM) with UV/H_2O_2 initiating system and evaluation of its application performance

Yongzhi Liu[a,b], Huaili Zheng[a,b,*], Bin Si[a,b], Yongjun Sun[c,d], Chun Zhao[a,b,e], Bincheng Xu[a,b], Xinyu Zheng[a,b]

[a]*Key Laboratory of the Three Gorges Reservoir Region's Eco-Environment, Ministry of Education, Chongqing University, Chongqing 400045, China, email: 1571709188@qq.com (Y. Liu), 1579505026@qq.com (B. Xu)*
[b]*National Centre for International Research of Low-carbon and Green Buildings, Chongqing University, Chongqing 400045, China, email: hlz6512@163.com (H. Zheng), 1096135337@qq.com (B. Si), 476997882@qq.com (X. Zheng)*
[c]*College of Urban Construction, Nanjing Tech University, Nanjing, 211800, China, email: 776425085@qq.com (Y. Sun)*
[d]*Jiangsu Key Laboratory of Industrial Water-Conservation & Emission Reduction, College of Environment, Nanjing Tech University, Nanjing, 211800, China*
[e]*College of Water & Architectural Engineering, Shihezi University, Shihezi 832000, China, email: 48610117@qq.com (C. Zhao)*

Received 28 October 2017; Accepted 19 March 2018

ABSTRACT

Ultraviolet (UV) initiation polymerization has been attracted great attention from researchers in the field of water and wastewater treatment. In this study, polyacrylamide (PAM) was successfully synthesized by the UV/H_2O_2 system and was characterized by FTIR, ^{1}H NMR, ^{13}C NMR, TG/DSC and SEM. SEM analysis results revealed that the synthesized PAM by UV/H_2O_2 initiation had different surface structures compared with commercial PAM. The study on factors affecting PAM intrinsic viscosity showed that the optimum conditions for PAM synthesis by the UV/H_2O_2 initiation system were 600 μm/cm^2 UV-light intensity, 1.7 wt‰ H_2O_2, pH = 6.25 wt% acrylamide (AM), 30 min illumination time. The active radical for PAM polymerization by UV/H_2O_2 system was validated by adding methanol and tertbutyl alcohol (TBA) to quench hydroxyl the radicals (·OH). Evaluation of PAM flocculation performance by treating the kaolin suspension showed that the maximum turbidity removal by the synthesized PAM was 95.4%, which was greatly superior to the commercial PAM.

Keywords: Polyacrylamide; UV/H_2O_2; Hydroxyl radical; Intrinsic viscosity; Flocculation

1. Introduction

Industrial and municipal wastewater contains large amounts of fine suspended solids, colloidal solids, inorganic particles, organic particles and other contaminants, which cause serious pollution to water environment [1]. To remove these particles, various technologies have been developed such as membrane filtration, precipitation, adsorption, coagulation, flocculation, electrolytic methods et al. [2]. Among these technologies, coagulation/flocculation is a very common and important purification technique to remove colloids and suspended particles from water [3,4]. During coagulation process, the flocculant interacts with tiny particles by means of charge neutralization, electrostatic patch, polymer bridging, and sweep flocculation. Thus, microscopic particles in water were destabilized and then separated from wastewater [5]. The performance of flocculation seriously depends on the properties of flocculants [6]. Therefore, it is of great significance for grafting of polyacrylamide chains (PAM) onto the backbone of performed polymer which obtain copolymer with non-toxic, bio-degradable merits [7,8]. And it has received great attention due to their high efficiency and environment-friendly requirement. Commonly, synthetic polymeric flocculants are based on polyacrylamide (PAM) or its derivatives because of their perfect flocculation effect and low economic costs [4]. Moreover, the monomer of PAM is acrylamide (AM) with the highest k_p/k_t constant in all known

*Corresponding author.

monomers, where k_p and k_t stand for the rate constant for chain propagation and chain termination of radical polymerization, respectively. AM is the most reactive monomers to undergo radical polymerization thus build up extra-high molecular weight [9]. These years, many studies based on PAM have been explored. Lee et al., synthesized a ferric chloride-polyacrylamide hybrid polymer and flocculation experiment results showed that more than 99% of turbidity, 89% of COD and 99% of color were removed for kaolin suspension and Terasil Red *R* wastewater, respectively [10]. Li et al., synthesized a copolymer of acrylamide and acryloylamino-2-hydroxypropyl trimethyl ammonium chloride and flocculation experimental results demonstrated a superiority of the copolymer product under both neutral and alkaline conditions [11]. Rani et al., studied the polyacrylamide grafted gum ghatti, which exhibited a high flocculation efficacy on kaolin suspension and municipal wastewater [12].

Generally, PAM is synthesized through thermal induced solution polymerization in industrial production because solution polymerization is simple and practicable [13]. Nevertheless, traditional thermal initiation-based polymerizations are always severe on the reaction temperature and need a long reaction time [14]. Recent years, ultraviolet (UV) initiation based aqueous solution polymerization has received great attention because it is environment-friendly, easy to control, fast, and energy-efficient [15]. UV initiation-based polymerizations are tolerant on polymerization temperature, which can implement at room temperature or even lower [16]. Besides, UV irradiation can realize the surface modification to improve the flocculation efficiency [17]. Thus far, most investigations about the UV/H_2O_2 system and the Fe^{2+}/H_2O_2 system are to degrade refractory organics using generated hydroxyl radicals (·OH) [18–21]. Moreover, some researchers have studied the polymer synthesis using ·OH as initiation radical generated from UV/H_2O_2 or Fe^{2+}/H_2O_2 system. D. Trimnell et al. have used the Fe^{2+}/H_2O_2 system as an initiator to synthesize graft copolymer of methyl acrylate onto granular cornstarch [22]. Kubota et al. have synthesized a poly (N-isopropyl acrylamide) gels by the UV/H_2O_2 process [23]. However, there are few works about exploring the UV/H_2O_2 or Fe^{2+}/H_2O_2 system as an initiator to synthesize organic polymeric flocculants and the flocculation performance of the synthesized flocculants.

This study investigated the optimized synthesis of the PAM using the UV/H_2O_2 system as an initiator and evaluated its flocculation performance of the synthesized flocculants. The synthesized PAM was characterized by Fourier transform infrared spectroscopy (FTIR), ^{1}H NMR spectrum, ^{13}C NMR spectrum, scanning electron microscopy (SEM) and thermal analysis (TG/DSC). Several factors influencing the PAM intrinsic viscosity such as UV intensity, H_2O_2 concentration, initial pH value, and monomer (AM) concentration were studied to optimize the PAM synthesis. Methyl alcohol and tertbutyl alcohol (TBA) were used to determine the key active radical of PAM polymerization in UV/H_2O_2 system and then the possible polymerization mechanism was presented on the basis. Finally, flocculation performance of the synthesized PAM was evaluated by flocculation test using kaolin suspension as target turbidity matters. Our findings suggested that the UV/H_2O_2 system in this work could act as an efficient initiator with some advantageous properties, including short reaction time, high intrinsic viscosity, with no need for deoxygenating and excellent flocculation performance, which may attract great attention as a promising technology for polymer material synthesis. For example, some natural organic polymer flocculants have gained increasing concern due to their environmental friendship, no secondary pollution, and renewability [24–26]. However, some inherent drawbacks of these natural organic polymer flocculants such as relatively low intrinsic viscosity, will cause poor flocculation performance [27]. Therefore, our suggested synthesis method could be used for modifying natural copolymer flocculants to get better flocculation performance.

2. Materials and methods

2.1. Materials and equipment

Reagents used in this study are as follows: AM (99.0% wt. Chongqing Lanjie Tap Water Company, Chongqing, China), H_2O_2 (30% wt. Chongqing Chuandong Chemical Reagent Co. Ltd, Chongqing, China). All solutions in this study were prepared with ultrapure water (GWA-UN, General, Beijing, China). Fig. 1 shows a schematic of the experimental setup, which was composed of a water-cooled 500W high-pressure Hg lamp assembly (main radiation wavelength, 365 nm) and four reaction vessels (Pyrex glass) coupled with four rotated platforms. The high-pressure Hg lamp was powered by a DC adjustable power supply (Jiguang Special Lighting Electrical Factory, Shanghai, China). UV irradiation intensity was measured by an ultraviolet radiation meter (UV-A, HANDY, Beijing Normal University Photoelectric Instrument Factory, China).

2.2. Synthesis of polyacrylamide (PAM)

Predetermined amounts of AM, H_2O_2, and ultrapure water were added to Pyrex glass vessel and then stirred until full blending. The initial pH of the reaction liquid was adjusted with both hydrochloric acid (0.1 mol/L) and sodium hydroxide (0.1 mol/L). Subsequently, the reaction vessels were exposed to UV irradiation at room temperature until the required reaction time. During experiments, reaction vessels were set on the rotating platform with a rotation speed of 8 rpm to make vessels receive UV-light regularly. UV irradiation intensities around reaction ves-

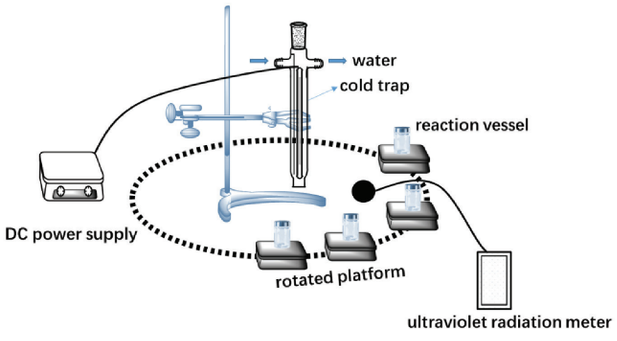

Fig. 1. Schematic of the experimental setup.

sels were measured and controlled using the ultraviolet radiation meter by adjusting the distance between reaction vessels and the high-pressure Hg lamp. The reaction temperature was maintained at room temperature. After polymerization, the synthesized PAM gels were aged for 2 h and then washed several times using ethanol and soaked for 24 h to remove the residual monomer in the polymerization reaction. Finally, the product was dried in a vacuum oven at 60°C until constant weight is obtained.

2.3. Characterization of the synthesized PAM

The FTIR spectra of the synthesized PAM was acquired using KBr pellets on a 550 Series II infrared spectrometer (Bruker Company, Switzerland) with wave numbers from 500 to 4000 cm^{-1}. The ^{1}H NMR and ^{13}C NMR spectra of the PAM were obtained by an advance 500 NMR spectrometer (Bruker Company, Germany) in deuterium oxide (D_2O) as a solvent with tetramethylsilane as an internal standard. The thermal stability of the PAM (TG/DSC) was determined by a TG/DSC/1100LF instrument (Mettler, Switzerland) under argon atmosphere from 20°C to 600°C at a heating rate of 10°C/min. The SEM images of the PAM were acquired by MIRA 3 LMH (Tescan Trade, Shanghai) instrument to investigate its surface morphology.

2.4. Measurement of intrinsic viscosity

The intrinsic viscosity of the synthesized PAM was measured by the One Point Method [20] to stand for the size of the viscosity average molecular weight of PAM. The intrinsic viscosity of PAM was determined using Ubbelohde capillary viscometer (Shanghai Shenyi Glass Instrument Co., Ltd., China) at 30 ± 0.05°C. The molecular weight of the polymers were calculated according to their intrinsic viscosities, and the calculation equation was Formula (1) according to the Chinese Standard (GB/T 12005.10-1992), as follows:

$$M_r = 802[\eta]^{1,25} \quad (1)$$

In this formula, M_r is the viscosity average molecular weight, [η] is the intrinsic viscosity (mL/g).

2.5. Flocculation performance

Three PAM samples with different synthesis conditions and intrinsic viscosity were chosen as flocculants to investigate their flocculation performance on kaolin suspension. The three different PAM samples were named as PAM_1, PAM_2, and PAM_3, respectively and their detailed information is listed in Table 1.

The kaolin suspension was prepared as target turbidity. The concentration and volume of the simulated kaolin suspension are 0.3 g/L and 500 mL, respectively. The initial pH of the kaolin suspension was adjusted with both hydrochloric acid (0.1 mol/L) and sodium hydroxide (0.1 mol/L). Flocculation tests were performed once the predetermined concentration PAM (1 mg/L) was added to the simulated kaolin suspension on a program-controlled jar test apparatus (TA6, Hengling Technology Co., Ltd, China). The coagulation procedure includes three steps: rapid stirring at 120 rpm for 2 min, stirring at a medium speed of 40 rpm for 5 min, slow stirring at 10 rpm for 6 min. After, the formed flocs free settled for 30 min. Then the turbidity of kaolin suspension at depth 2 cm below the liquid surface was measured with a HACH (HACH 2100Q, American Hach Company) turbidity meter.

Table 1
Samples of PAM

Samples	Intrinsic viscosity (mL/g)	Molecular weight	The source of product	AM concentration
PAM_1	800	3412218	Commercial product	–
PAM_2	838	3616008	Synthesized product	25 wt%
PAM_3	1638	8357314	Synthesized product	25 wt%

3. Results and discussion

3.1. Characterization of the synthesized PAM

3.1.1. FTIR spectra analysis

Fig. 2 illustrates the FTIR spectra of the synthesized PAM, which is coincident with the results of Li and Sadeghalvaad's works [28,29]. The absorption peaks at 3442 cm^{-1} and 1649 cm^{-1} were attributed to the stretching vibration of amino groups ($–NH_2$) and carbonyl groups (C = O) of amide in PAM according to Wang et al. [29–31]. The slight peak at 2926 cm^{-1} was assigned to asymmetric stretching vibration of methylene ($–CH_2$) according to Wang et al. [32]. The absorption peaks at 1454 cm^{-1} were due to the C–N stretching vibration, 1319 cm^{-1} was due to the C–H bending vibration, and 1189 cm^{-1} was for the $–NH_2$ bending vibration [28]. Accord-

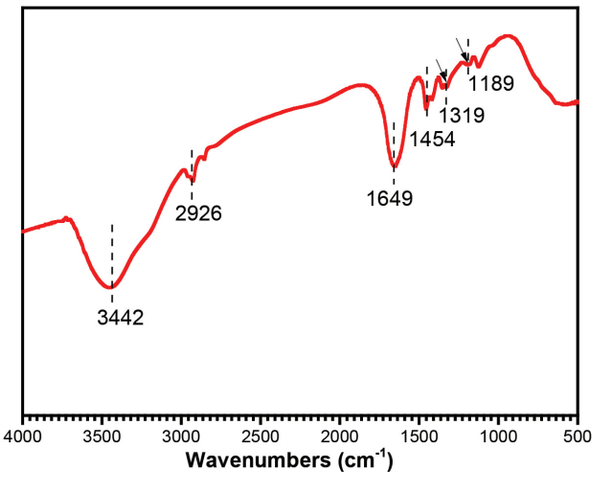

Fig. 2. FTIR spectra of the synthesized PAM.

ing to the works by Guan et al. [30], the absorption peaks at 1432 and 985 cm^{-1} stands for $=CH_2$ and =CH double bonds, respectively. However, they were not found in we synthesized PAM spectrum, which indicated the carbon-carbon double bonds cleaved during the polymerization reaction. In conclusion, the FTIR spectrum implied that we synthesized PAM had the same functional group constitution with other works.

3.1.2. ^{1}H NMR spectrum analysis

The ^{1}H NMR spectrum analysis was performed to further study the molecular structures of the synthesized PAM. As shown in Fig. 3, the strong peak at δ = 4.77 ppm is ascribed to the solvent proton of deuteroxide (D_2O) [14]. The asymmetric peaks at δ = 1.63 ppm and δ = 2.17 are attributed to the protons of methylene ($–CH_2$) and methane (–CH) groups, respectively [33,34]. Hence, the ^{1}H NMR spectrum suggested that we synthesized PAM had the same Hydrogen spectral series with others.

3.1.3. ^{13}C NMR spectrum analysis

Fig. 4 shows the ^{13}C NMR spectra of the synthesized PAM. The characteristic peak observed at 35.11 ppm was attributed to the backbone $–CH_2–$ (a) group [35]. The resonance peak at 41.93 ppm represented the carbon signal from –CH– (b) group [36]. Meanwhile, the peak at 179.66 ppm was characteristic signal peak of C = O (c) group [37]. It provided another evidence for the successful synthesis of PAM.

3.1.4. TG/DSC analysis

Thermal analysis was performed to investigate the thermal stability of we synthesized PAM and the results are shown in Fig. 5, which demonstrates that there are three main stages of thermal decomposition. In the first stage, weight loss of about 14% in the range of 50–100°C was due to the loss of absorbed water [14,38]. In the second stage,

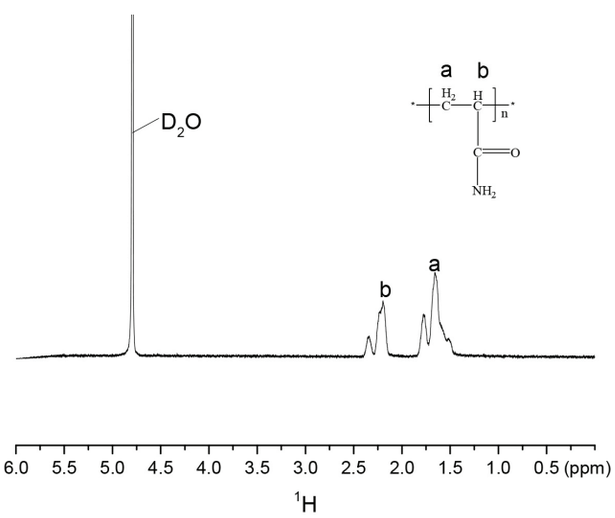

Fig. 3. ^{1}H NMR spectrum of the synthesized PAM.

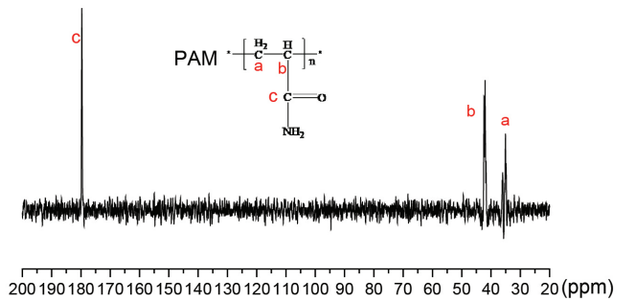

Fig. 4. ^{13}C NMR spectrum of the synthesized PAM.

weight loss of about 15% within the range of 170–336°C was ascribed to the thermal decomposition and imidization of amide groups (–CO–NH–) [39]. In the final stage, the thermal decomposition was found at above 336°C and weight loss of about 60% was due to the thermal decomposition of the PAM backbone [40]. The synthesized PAM decomposed completely above 500°C and the residual weight percentage was about 10%. Therefore, the TG/DSC analysis indicated that the synthesized PAM by the UV/H_2O_2 initiation system had an excellent thermal stability.

3.1.5. SEM images analysis

SEM images and calculated fractal dimension are illustrated in Fig. 6, which directly show the surface morphology of PAM. As shown in Fig. 6a, the commercial PAM has a regular structure with smooth surface morphology. Whereas the synthesized PAM (Fig. 6b) exhibits a more folded structure. In addition, Image-Pro Plus 6.0 software was used to calculate the fractal dimension which could be a proof to further investigate the surface morphology [39,41]. The average fractal dimensions of the commercial PAM and the synthesized PAM are 1.25 and 1.30, respectively. The results indicated that the commercial PAM and the synthesized PAM had different morphological structures. According to the works by Li et al., UV initiation system could modify the surface of organic polymer flocculants [41]. Hence, the

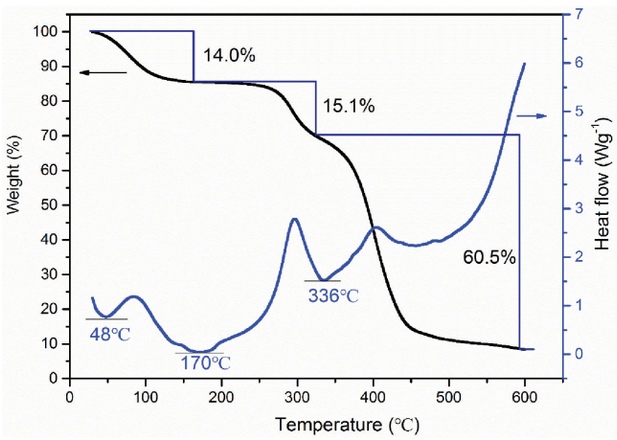

Fig. 5. TG/DSC analysis of the synthesized PAM.

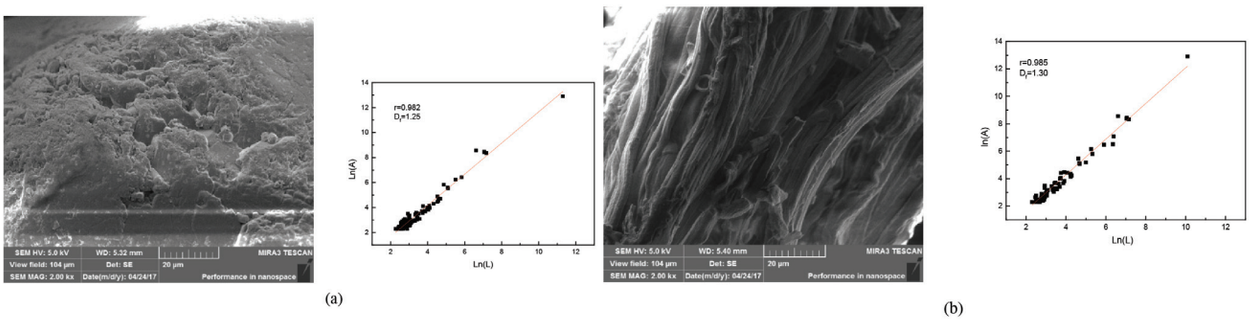

Fig. 6. SEM micrographs of (a) PAM1 and (b) PAM2.

results demonstrated that the UV/H_2O_2 initiation system could similarly modify morphological characteristics of the PAM surface.

3.2. The effect of synthesis conditions on PAM intrinsic viscosity

3.2.1. The effect of UV-light intensity

Fig. 7 shows the effect of UV-light intensity on intrinsic viscosity of the PAM. The PAM intrinsic viscosity as a function of illumination time under different UV-light intensities exhibits a similar variation trend. As shown in Fig. 7, the PAM intrinsic viscosity increases with increased illumination time at the initial stage under any UV-light intensity. However, the PAM intrinsic viscosity begins to decrease gradually when the illumination time exceeds some value. This could be explained as that the polymerization initiated by the UV/H_2O_2 system followed the radical polymerization mechanism [42]. Hydroxyl radicals (·OH) could continually be generated in the UV/H_2O_2 initiation system. These generated hydroxyl radicals could react with monomers

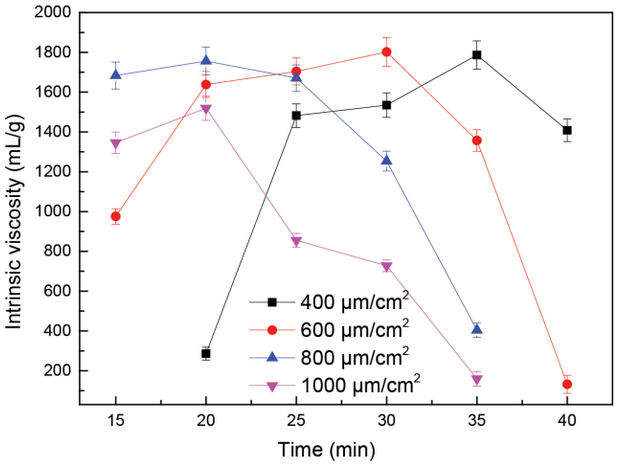

Fig. 7. Effect of UV light intensity on PAM intrinsic viscosity. Experimental condition: [AM] = 25 wt%, [H_2O_2] = 1.7 wt‰ and initial pH = 6.

(AM) according to Eq. (5) and then generated the macroradicals (M_i) [23]. At the early stage of the reaction, the M_i and the *AM* were more likely to collide with each other because the concentration of *AM* was relatively high and thus facilitated the growth of molecular chains [43]. Results showed that *AM* concentration decreased slightly as time increased while the concentration of free radicals increased with time. The collision rate between M_i and free radicals (including M_i itself) became higher and this may terminate the chain propagation reaction of M_i [Eq. (9)] so that impeded the growth of PAM intrinsic viscosity [44]. Moreover, the chain propagation was hindered with intrinsic viscosity increasing because it would be harder for ·OH and M_i to colloid with each other when liquid was viscous. Hence, the intrinsic viscosity of the PAM increased with the increased illumination time until reached a maximum value. Furthermore, with illumination time continue increasing, PAM intrinsic viscosity decreased gradually because of the intermolecular cross link reaction and gel effect [43]. There were some insoluble substances of undissolved PAM if the reaction time was longer than the time reaching maximum intrinsic viscosity under different light intensity. For example, we found a lot of insoluble substances when dissolving the PAM (600 μm/cm²) with the synthesis time of 35 min or longer. However, there was nearly no insoluble substance founded for PAM with shorter reaction time.

Fig. 7 also shows that the maximum PAM intrinsic viscosities are similar under different UV-light intensities of 400 μm/cm², 600 μm/cm² and 800 μm/cm². However, the maximum PAM intrinsic viscosity under 1000 μm/cm² is lower than other light intensities. This might because the radical concentration was applicable for the polymerization reactions when the UV-light intensity was between 400 and 800 μm/cm². And it was other factors such as the monomer concentration that determined the maximum PAM intrinsic viscosity. When the UV-light intensity was 1000 μm/cm², the really high UV-light intensity would bring about cross-linking reaction in a short time because of the excess ·OH generated under 1000 μm/cm². In addition, the reaction time for reaching the maximum intrinsic viscosity for 400, 600, and 800 μm/cm² was 35, 30, and 20 min. This phenomenon was attributed to the fact that the initial rate of free radical polymerization by photo-initiation was directly proportional to the incident light intensity [44]. More free

radicals would generate with UV-light intensity increasing and then caused the increase of polymerization rate.

3.2.2. The effect of H_2O_2 concentration

Initiator concentration is a very important parameter in UV initiation process [45]. To study the effect H_2O_2 concentration on PAM intrinsic viscosity, a series of experiments with different H_2O_2 concentrations were conducted and the results are shown in Fig. 8. The variation curves that the intrinsic viscosity as a function of illumination time for different H_2O_2 concentration are similar. However, the optimal illumination time was 30 min for 1.5 wt‰, 1.7 wt‰, and 1.9 wt‰ H_2O_2 concentration, 20 min for 2.5 wt‰ H_2O_2 concentration. This was ascribed to the primary radical concentrations, which seriously increased with H_2O_2 concentration increasing. The increasing primary radical concentration resulted in the faster polymerization rate and then shorten the time to reach the maximum intrinsic viscosity [46]. Moreover, PAM maximum intrinsic viscosity increased with H_2O_2 concentration increasing until 1.7 wt‰. When H_2O_2 concentration rose to 1.9 wt‰, PAM maximum intrinsic viscosity began to decrease. This phenomenon was because H_2O_2 was the reactive center of the polymerization reaction. The chains propagation rate increased with H_2O_2 concentration increasing, which was higher than chains termination and chains transfer rate and then enhanced PAM intrinsic viscosity [47]. However, When H_2O_2 concentration rose to 1.9 wt‰, chains termination and chains transfer rate became so high that hindered chains propagation reactions and then affect PAM intrinsic viscosity. On the other hand, the excess ·OH would rapidly react with monomers to produce a lot of heat and then aggravate the gel effect [43].

3.2.3. The effect of initial pH value

Fig. 9 shows that the initial pH is an important parameter for PAM synthesis. In detail, the maximum intrinsic viscosity was 1581 mL/g, 1676 mL/g, 1802 mL/g, and 1465 mL/g, 1475 mL/g, wherein the pH was 2, 4, 6, 8 and 10 respectively. It is clear that PAM maximum intrinsic viscosity was distinctly higher at faintly acid synthesis condition (pH 4, 6) than strong acid or alkaline condition (pH 2, 8, 10). This phenomenon can be explained as follows: (1) In the UV/H_2O_2/PAM heterogeneous system, the amount of OH radicals decrease because they can easily react with OHH^- anions which are major decomposition product of H_2O_2 in alkaline conditions [48]. Therefore, the maximum intrinsic viscosity in alkaline conditions was lower than that in other designed pH values. (2) Intramolecular and intermolecular imidization was more likely to occur between acrylamide molecules in strong acid environment (pH < 4). This side reaction could produce the cross-linked and highly branched PAM [49]. In addition, in the UV/H_2O_2/PAM heterogeneous system, pH may also influence the production of hydroxyl radicals by changing the surface charge and the adsorption of radical scavenger [50]. The strong acid environment may inhibited the adsorption of H_2O_2 on PAM surface, causing the decrease of OH radicals [51]. These reasons resulted in PAM intrinsic viscosity decreasing. Consequently, the optimum pH was supposed to be faintly acid (pH = 4–6).

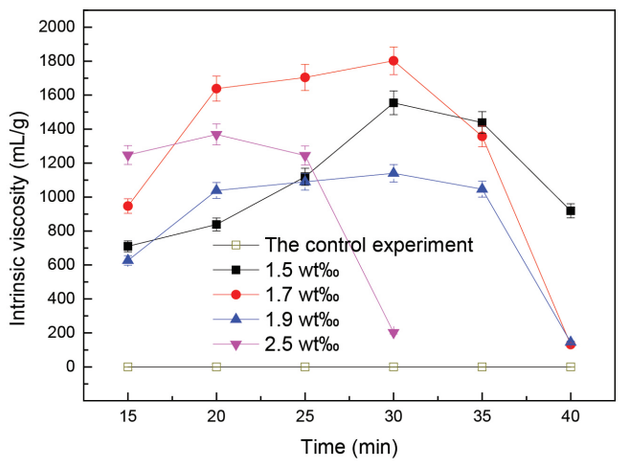

Fig. 8. Effect of H_2O_2 concentration on PAM intrinsic viscosity. Experimental condition: [AM] = 25 wt%, [light intensity] = 600 μm/cm² and initial pH = 6. The control experiment ([H_2O_2] = 0).

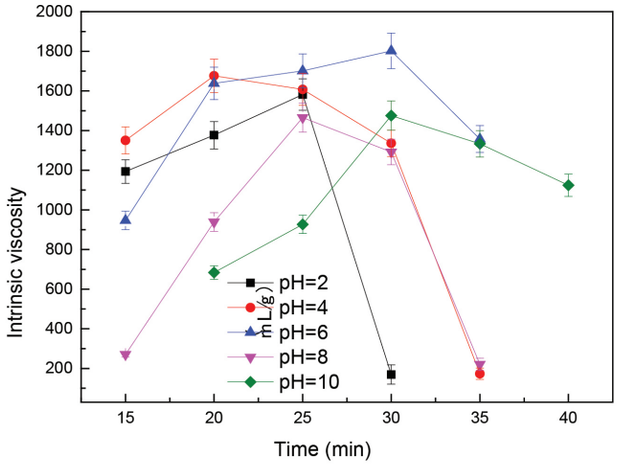

Fig. 9. Effect of pH on PAM intrinsic viscosity. Experiment condition: [AM] = 25 wt%, [H_2O_2] = 1.7 wt‰, [light intensity] = 600 μm/cm².

3.2.4. The effect of monomer concentration

The PAM maximum intrinsic viscosity was 1213 mg/L, 1639 mg/L, 1802 mg/L, 1653 mg/L, 1426 mg/L, wherein the corresponding monomer concentration was from 15 wt% to 35 wt% and illumination time was 35 min, 30 min, 30 min, 25 min and 20 min respectively. The PAM intrinsic viscosity gradually decreased after reaching the maximum value because the chain termination reaction and cross-link reaction stopped chain propagation and then caused the poor solubility of PAM. In addition, the polymerization rate of AM in UV/H_2O_2 system was proportional to the first order of the monomer concentration (AM) based on the classical radical polymerization mechanism [52]. Therefore, the illumination time for reaching the maximum intrinsic viscosity decreased with monomer concentration increasing (Fig.10).

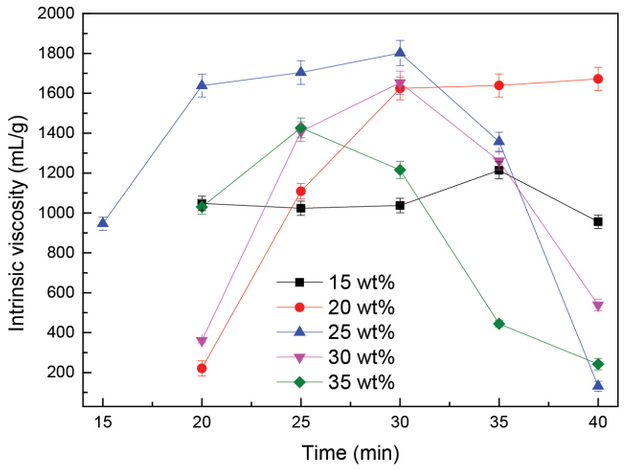

Fig. 10. Effect of monomer concentration on PAM intrinsic viscosity. Experimental condition: [H_2O_2] = 1.7 wt‰, [light intensity] = 600 μm/cm^2 and initial pH = 6.

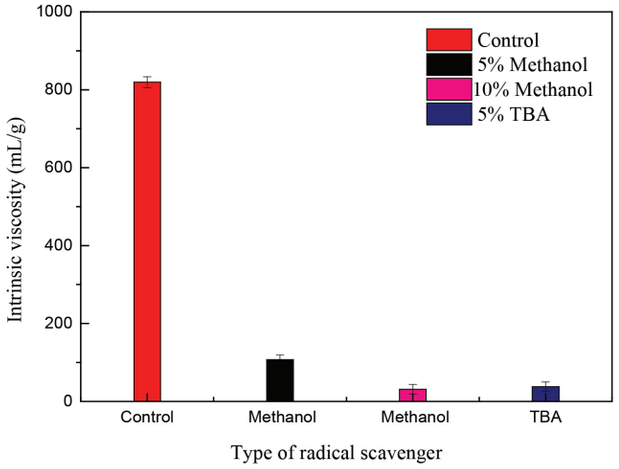

Fig. 11. Effect of methanol and TBA content on PAM intrinsic viscosity. Experimental condition: [AM] = 25 wt%, [H_2O_2] = 1.5 wt‰, pH = 6 and illumination time 30 min.

When the monomer concentration was 15 wt%, it needed at least 20 min to synthesis the PAM gel and its intrinsic viscosity was lower than other groups. This was because the monomer concentration was at an extremely low level so that the probability of collision between primary radical and monomer molecules was low extreme due to the cage effect [47]. With monomer concentration increasing, the cage-effect became weak so that PAM intrinsic viscosity increased gradually. However, the PAM intrinsic viscosity was distinctly decreased when the monomer concentration rose to 30 wt% and 35 wt%. This phenomenon was because the chain termination reaction and chain transfer reaction were more likely to occur when the monomer concentration was relatively higher and then resulted in the decrease of intrinsic viscosity [53,54]. Therefore, the optimum monomer concentration was supposed to be 20–30 wt%.

3.3. The mechanism for UV/H_2O_2 system to synthesize PAM

The mechanism for UV/H_2O_2 system to synthesize PAM was supposed to be free radical polymerization mechanism [23,43]. Hydroxyl radical, which generated from UV-light initiated H_2O_2 decomposition, was the primed radical. To validate this point, PAM polymerization experiments without UV-light radiation or H_2O_2 addition were conducted. PAM colloids were both not synthesized as expected. We could conclude that UV-light and H_2O_2 were both necessary for PAM polymerization. In addition, the synthesis method could realize polymerization without deoxygenating by bubbling with N_2, which was due to the fact that UV/H_2O_2 system could produce OH radicals even when oxygen existence [51,55]. Moreover, methanol and tert butyl alcohol (TBA), which are always recognized as hydroxyl radical scavengers [55,56], was applied to validate the crucial role of hydroxyl radicals. As shown in Fig. 11, the addition of methanol and TBA observably brought down the PAM intrinsic viscosity, which revealed that ·OH was the key for PAM polymerization in the UV/H_2O_2 initiation system.

Therefore, the probable mechanism for UV/H_2O_2 system to synthesize PAM could be presumed as follows: Hydroxyl radicals were generated from UV light initiated H_2O_2 and then AM interacted with ·OH generating the AM macroradicals. The generated AM macroradicals further reacted with AM and then form PAM high polymers. The polymerization reaction mechanism is demonstrated as Eqs. (1)–(9). In the UV/ H_2O_2 system, the reaction (1–4) is commonly occurred [19,21,57]. However, the possibility of reaction (2–4) is negligibly low in polymerization reaction [23]. Therefore, reaction (1) is the main reaction generating ·OH to initiate monomer polymerization. Summarily, the polymerization mechanism for UV/H_2O_2 initiation system was shown as follows:

Formation of free radical

$$H_2O_2 + hv \rightarrow \cdot OH + \cdot OH \quad (1)$$

$$\cdot OH + H_2O_2 \rightarrow H_2O + HO_2 \cdot \quad (2)$$

$$HO_2 + H_2O_2 \rightarrow H_2O + O_2 + \cdot OH \quad (3)$$

$$2HO_2 \cdot \rightarrow H_2O_2 + O_2 \quad (4)$$

Initiation

$$M + \cdot OH \rightarrow M_i \quad (5)$$

M = monomer, M_i = monomer macroradical

Propagation

$$M_i + M \rightarrow M_2 \quad (6)$$

$$M_{n-1} + M \rightarrow M_n \quad (7)$$

Transfer

$$M_n + M \rightarrow P_n + M \quad (8)$$

Termination

$$M_n + M_i \rightarrow P_{n-1}(polymer) \quad (9)$$

3.8. Evaluation of flocculation performance of the PAM

To evaluate the flocculation performance of the synthesized PAM, a series of flocculation experiments was performed. Kaolin suspension was chosen as the turbidity donor because of its widely used to simulate high turbidity wastewater [15,58]. Fig. 12a shows the effect of PAM dosage on turbidity removal at pH = 7. The turbidity removal efficiency for PAM_1, PAM_2 and PAM_3 had a similar variation tendency, which increased with PAM dosage increasing, but began to decrease after reaching a specific value (1 mg/L for PAM_3; 4 mg/L for PAM_1 and PAM_2). The similar variation tendency for PAM_1, PAM_2, and PAM_3 was because the surface of PAM was insufficient to adsorb colloid particles effectively when PAM dosage was low. While excess PAM dosage would cause cage effect, which restrained the growth of flocs thereby reduced the turbidity removal and settling efficiency

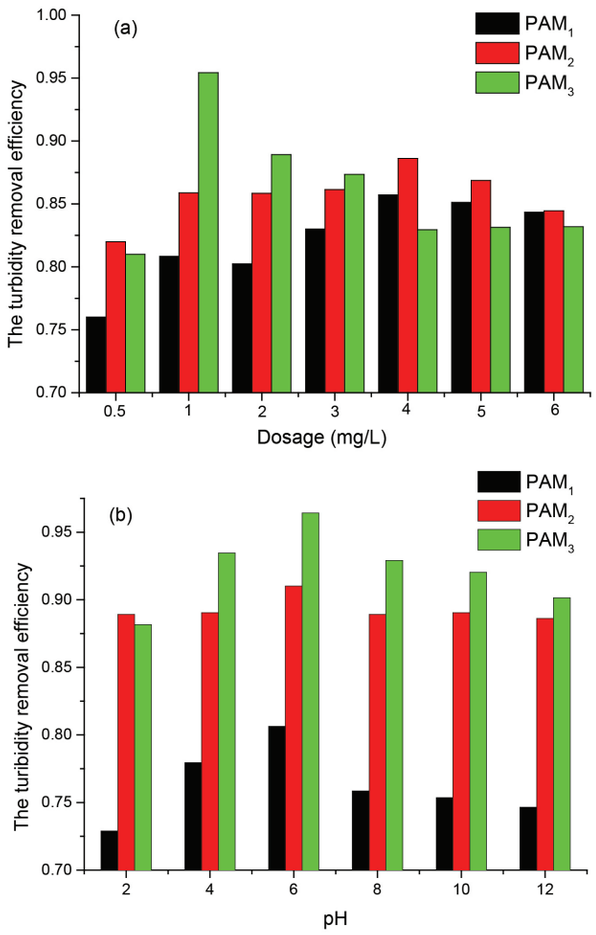

Fig.12. Effect of (a) PAM dosage and (b) pH value on PAM flocculation efficiency. Experimental condition for (a): [kaolin] = 0.3 g/L, initial pH = 7; experimental condition for (b): [kaolin] = 0.3 g/L, [PAM dosage] = 1 mg/L.

[59]. It should be noted that the maximum turbidity removal for PAM_1, PAM_2, and PAM_3 was 83.0%, 89.9%, and 95.4% respectively when the dosage was 4, 4, and 1 mg/L. The flocculation efficiency for PAM_3 was obviously superior to PAM_1 and PAM_2, while the dosage for PAM_3 to reach the maximum turbidity removal was remarkably lower than PAM_1 and PAM_2. The considerably excellent performance for PAM_3 on turbidity removal was due to the fairly high intrinsic viscosity (1638 mL/g) of PAM_3, which could supply a large surface area resulting in intensifying of the adsorption bridging effect [60]. In addition, higher the intrinsic viscosity, longer will be the polymer chains. PAM_3 with the fairly high intrinsic viscosity (1638 mL/g) more likely to collide with kaolin particles and thence increase the flocculation performance. The result is in consistent with Singh's easy approachability model and Brostow, Pal and Singh's model of flocculation, which are suitable for acrylamide polymer flocculant [24,61,62]. Moreover, the flocculation efficiency for PAM_2, which had a similar molecular weight with the commercial PAM_1, was also superior to PAM_1. This was because the PAM_2 possessed a special surface morphological structure as shown in Fig. 6, which could enhance the bridging effect in flocculation processes. However, the flocculation efficiency of PAM_3 was lower than the others at 6 mg/L. For PAM_3 with higher intrinsic viscosity, it was more likely to result in the phenomenon of colloidal protection under excess dosage, in which kaolin colloidal surface will develop a macromolecular layer that stabilize and protect kaolin particles, which resulted poor flocculation efficiency [63]. In addition, the long chains of PAM_3 cannot stretch out entirely under high dosage, which could result in the cage effect that prevent the growth of flocs and reduce the settling efficiency [64].

In the flocculation process, pH was also a very important parameter affecting turbidity removal efficiency. Fig. 12b shows the effects of pH value on the turbidity removal of kaolin suspension. Results showed that the turbidity removal increased with increased pH until pH = 6 and then gradually decreased with further increased pH. This phenomenon was due to the hydrolysis of PAM. PAM existed mainly as the style of the molecule when the pH was below 4, which made PAM curl up together like coils so that resulted in the poor turbidity removal efficiency [58]. When pH value rose to 4–6, PAM macromolecular chains could sufficiently stretch due to hydrolysis, which could enhance the absorption of kaolin particles on PAM molecules so that resulted in a high turbidity removal efficiency [58]. However, the hydrolysis of PAM would aggravate with the pH value further increasing, which made PAM molecular chains possess many negative charges. Electrostatic repulsion between PAM molecular chains with many negative charges and kaolin particles resulted in poor flocculation performance [11,65]. In addition, the turbidity removal efficiency for the synthesized PAM_2 and PAM_3 was superior to the commercial PAM_1, which was due to the high intrinsic viscosity and special surface structure that made the synthesized PAM easier to generate dense and large flocs by adsorption bridging effect as shown in Fig. 13.

4. Conclusion

In this study, we investigated the method of UV/H_2O_2 photo-initiation polymerization using acrylamide as the

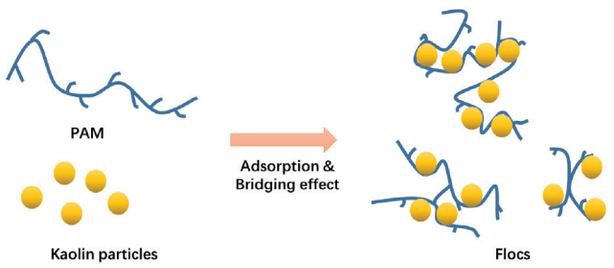

Fig. 13. Schematic of flocculation.

monomer. All the results of the experiments concluded that PAM could be synthesized by UV/H_2O_2 photo-initiation polymerization. Meanwhile, synthesis conditions affecting the PAM intrinsic viscosity and the PAM flocculation performance were studied. The main results of this study are as follows:

1. PAM was successfully synthesized by UV/H_2O_2 photo-initiation system and the structure of synthesized PAM was characterized by FTIR, ^{1}H, SEM and TG/DSC analysis.
2. Factors affecting the PAM intrinsic viscosity were studied and the results showed that UV light intensity, H_2O_2 concentration, monomer concentration, illumination time and initial pH had a great impact on PAM intrinsic viscosity.
3. The polymerization mechanism for the UV/H_2O_2 photo-initiation system to synthesize PAM was speculated to be a free radical polymerization mechanism.
4. Turbidity removal experiments of kaolin suspension showed that 95.4% turbidity removal was obtained with 1 mg/L of the synthesized PAM at pH = 6. The flocculation experiments demonstrated a superiority of the synthesized PAM by UV/H_2O_2 initiation over the commercial PAM.

In conclusion, UV/H_2O_2 photo-initiation polymerization is a novel and promising method for flocculants synthesis, which has a great significance on water and wastewater treatment. The further study on other types of flocculants synthesis and the dynamics of the UV/H_2O_2 photo-initiation polymerization will be useful for better understanding and application of this technology.

Acknowledgment

This work was supported by the National Natural Science Foundation of China (Project No. 21477010) and 111 Project (Project No. B13041).

References

[1] V.H. Dao, N.R. Cameron, K. Saito, Synthesis, properties and performance of organic polymers employed in flocculation applications, Polym. Chem. UK, 7 (2015) 11–25.
[2] R. Yang, H.J. Li, M. Huang, H. Yang, A.M. Li, A review on chitosan-based flocculants and their applications in water treatment, Water Res., 95 (2016) 59–89.
[3] S.L. Chai, J. Robinson, F.C. Mei, A review on application of flocculants in wastewater treatment, Process Saf. Environ., 92 (2014) 489–508.
[4] B. Bolto, J. Gregory, Organic polyelectrolytes in water treatment, Water Res., 41 (2007) 2301–2324.
[5] L. Besra, P. Ay, Flocculation and dewatering of kaolin suspensions with the help of a combination of polymeric flocculants and surface active substances, J. Exp. Anal. Behav., 103 (2015) 524–541.
[6] J.Q. Jiang, The role of coagulation in water treatment, Curr. Opin. Chem. Eng., 8 (2015) 36–44.
[7] P. Pal, J.P. Pandey, G. Sen, Synthesis of polyacrylamide grafted polyvinyl pyrrolidone (PVP-g-PAM) and study of its application in algal biomass harvesting, Ecol. Eng., 100 (2017) 19–27.
[8] C.J. Zou, M.H. Liang, X.L. Chen, X.L. Yan, -Cyclodextrin modified cationic acrylamide polymers for flocculating waste drilling fluids, J. Appl. Polym. Sci., 131 (2014) 93–98.
[9] L.H. Lu, Z.D. Pan, H. Nan, W.Q. Peng, A novel acrylamide-free flocculant and its application for sludge dewatering, Water Res., 57 (2014) 304–312.
[10] K.E. Lee, T.T. Teng, N. Morad, B.T. Poh, M. Mahalingam, Flocculation activity of novel ferric chloride-polyacrylamide ($FeCl_3$-PAM) hybrid polymer, Desalination, 266 (2011) 108–113.
[11] L.J. Wang, J.P. Wang, S.J. Yuan, S.J. Zhang, Y. Tang, H.Q. Yu, Gamma radiation-induced dispersion polymerization in aqueous salts solution for manufacturing a cationic flocculant, Chem. Eng. J., 149 (2009) 118–122.
[12] P. Rani, G. Sen, S. Mishra, U. Jha, Microwave assisted synthesis of polyacrylamide grafted gum ghatti and its application as flocculant, Carbohyd. Polym., 89 (2012) 275–281.
[13] Y.J. Sun, C.Y. Zhu, Y.H. Xu, H.L. Zheng, X.F. Xiao, G.C. Zhu, M.J. Ren, Comparison of initiation methods in the structure of CPAM and sludge flocs properties, J. Appl. Polym. Sci., 133 (2016).
[14] H.L. Zheng, J.Y. Ma, C.J. Zhu, Z. Zhang, L.W. Liu, Y.J. Sun, X.M. Tang, Synthesis of anion polyacrylamide under UV initiation and its application in removing Dioctyl phthalate from water through flocculation process, Sep. Purif. Technol., 123 (2014) 35–44.
[15] J.Y. Ma, J. Shi, H.C. Ding, G.C. Zhu, K. Fu, X. Fu, Synthesis of cationic polyacrylamide by low-pressure UV initiation for turbidity water flocculation, Chem. Eng. J., 312 (2017) 20–29.
[16] Y. Yagci, S. Jockusch, N.J. Turro, Photoinitiated polymerization: Advances, challenges, and opportunities, Macromolecules, 43 (2010) 6245–6260.
[17] Y. Liao, H.L. Zheng, Q. Li, Y. Sun, D. Li, W.W. Xue, UV-Initiated polymerization of hydrophobically associating cationic polyacrylamide modified by a surface-active monomer: A comparative study of synthesis, characterization, and sludge dewatering performance, Ind. Eng. Chem. Res., 53 (2014) 11193–11203.
[18] Y.Y. Chen, Y.L. Ma, J. Yang, L.Q. Wang, J.M. Lv, C.J. Ren, Aqueous tetracycline degradation by H_2O_2 alone: removal and transformation pathway, Chem. Eng. J., 307 (2016) 15–23.
[19] P.B.L. Chang, T.M. Young, Kinetics of methyl tert-butyl ether degradation and by-product formation during UV/Hydrogen Peroxide water treatment, Water Res., 34 (2000) 2233–2240.
[20] J.C. Arthur, O. Hinojosa, M.S. Bains, ESR study of reactions of cellulose with·OH generated by Fe^{2+} /H_2O_2, J. Appl. Polym. Sci., 12 (1968) 1411–1421.
[21] K.G. Linden, E.J. Rosenfeldt, S.W. Kullman, UV/H_2O_2 degradation of endocrine-disrupting chemicals in water evaluated via toxicity assays, Water Sci. Technol., 55 (2007) 313–319.
[22] D. Trimnell, G.F. Fanta, J.H. Salch, Graft polymerization of methyl acrylate onto granular starch: Comparison of the Fe^{2+}/H_2O_2 and ceric initiating systems, J. Appl. Polym. Sci., 60 (2015) 285–292.
[23] H. Kubota, A. Fukuda, Photopolymerization synthesis of poly (N-isopropylacrylamide) hydrogels, J. Appl. Polym. Sci., 65 (1997) 1313–1318.

[24] P. Pal, J.P. Pandey, G. Sen, Synthesis, characterization and flocculation studies of a novel graft copolymer towards destabilization of carbon nanotubes from effluent, Polymer, 112 (2017) 159–168.
[25] P. Pal, J.P. Pandey, G. Sen, Chapter 5-Synthesis and application as programmable water soluble adhesive of polyacrylamide grafted gum tragacanth (GT-g-PAM), Biopolymer Grafting, (2018) 153–203.
[26] P. Pal, P. Rani, S. Mishra, J.P. Pandey, G. Sen, Grafted cinnamic acid: A novel material for sugarcane juice clarification (Chapter No. 13), Research Methodology in Food Sciences Integrated Theory and Practice, CRC Publications, (2017).
[27] J. Wang, Y. Chen, S. Yuan, G. Sheng, H. Yu, Synthesis and characterization of a novel cationic chitosan-based flocculant with a high water-solubility for pulp mill wastewater treatment, Water Res., 43 (2009) 5267–5275.
[28] M. Sadeghalvad, S. Sabbaghi, The effect of the TiO_2/polyacrylamide nanocomposite on water-based drilling fluid properties, Powder Technol., 272 (2015) 113–119.
[29] X. Li, H.L. Zheng, B.Y. Gao, Y.J. Sun, B.Z. Liu, C.L. Zhao, UV-initiated template copolymerization of AM and MAPTAC: Microblock structure, copolymerization mechanism, and flocculation performance, Chemosphere, 167 (2017) 71–81.
[30] Q.Q. Guan, H.L. Zheng, J. Zhai, B.Z. Liu, Y.J. Sun, Y.L. Wang, Z.N. Xu, C. Zhao, Preparation, characterization, and flocculation performance of P(acrylamide-co-diallyldimethylammonium chloride) by UV-initiated template polymerization, J. Appl. Polym. Sci., 132 (2015) 41747.
[31] L.J. Wang, J.P. Wang, S.J. Zhang, Y.Z. Chen, S.J. Yuan, G.P. Sheng, H.Q. Yu, A water-soluble cationic flocculant synthesized by dispersion polymerization in aqueous salts solution, Sep. Purif. Technol., 67 (2009) 331–335.
[32] H.L. Wang, J.Y. Cui, W.F. Jiang, Synthesis, characterization and flocculation activity of novel $Fe(OH)_{(3)}$-polyacrylamide hybrid polymer, Mater. Chem. Phys., 130 (2011) 993–999.
[33] D. Sasmal, R.P. Singh, T. Tripathy, Synthesis and flocculation characteristics of a novel biodegradable flocculating agent amylopectin-g-poly (acrylamide-co-N-methylacrylamide), Colloids Surfaces A: Physicochem. Eng. Asp., 482 (2015) 575–584.
[34] B.Z. Liu, H.L. Zheng, X.R. Deng, B.C. Xu, Y.J. Sun, Y.Z. Liu, J.J. Liang, Formation of cationic hydrophobic micro-blocks in P (AM-DMC) by template assembly: characterization and application in sludge dewatering, RSC Adv., 7 (2017) 6114–6122.
[35] L. Feng, H.L. Zheng, B.Y. Gao, S.S. Zhang, C.L. Zhao, Y.H. Zhou, B.C. Xu, Fabricating an anionic polyacrylamide (APAM) with an anionic block structure for high turbidity water separation and purification, RSC Adv., 7 (2017) 28918–28930.
[36] H.L. Zheng, L. Feng, B.Y. Gao, Y.H. Zhou, S.S. Zhang, Effect of the cationic block structure on the characteristics of sludge flocs formed by charge neutralization and patching. Materials, 10 (2017) 487.
[37] Z.H. Huang, Q.L. Wu, S.X. Liu, T.L. Liu, B. Zhang, A novel biodegradable βcyclodextrin-based hydrogel for the removal of heavy metal ions, Carbohyd. Polym., 97 (2013) 496–501.
[38] A. Sand, M. Yadav, D.K. Mishra, K. Behari, Modification of alginate by grafting of N-vinyl-2-pyrrolidone and studies of physicochemical properties in terms of swelling capacity, metal-ion uptake and flocculation, Carbohyd. Polym., 80 (2010) 1147–1154.
[39] C.L. Zhao, H.L. Zheng, L. Feng, Y.L. Wang, Y.Z. Liu, B.Z. Liu, B. Djibrine, Improvement of sludge dewaterability by ultrasound-initiated cationic polyacrylamide with microblock structure: The role of surface-active monomers, Materials, 10 (2017) 282.
[40] Y.J. Sun, C.Y. Zhu, W.Q. Sun, Y.H. Xu, X.F. Xiao, H.L. Zheng, H.F. Wu, C.Y. Liu, Plasma-initiated polymerization of chitosan-based CS-g-P(AM-DMDAAC) flocculant for the enhanced flocculation of low-algal-turbidity water, Carbohyd. Polym., 164 (2017) 222–232.
[41] X. Li, H.L. Zheng, Y.L. Wang, Y.J. Sun, B.C. Xu, C.L. Zhao, Fabricating an enhanced sterilization chitosan-based flocculants: Synthesis, characterization, evaluation of sterilization and flocculation, Chem. Eng. J., 319 (2017) 119–130.
[42] F.S. Dainton, M. Tordoff, The polymerization of acrylamide in aqueous solution, Trans. Faraday Soc., 53 (1957) 499–511.
[43] H.L. Zheng, Y.J. Sun, C.J. Zhu, J.S. Guo, C. Zhao, Y. Liao, Q.Q. Guan, UV-initiated polymerization of hydrophobically associating cationic flocculants: Synthesis, characterization, and dewatering properties, Chem. Eng. J., 234 (2013) 318–326.
[44] L.Y. Liu, Z.X. Zhang, W.T. Yang, Photoinitiated inverse emulsion polymerization of sodium acrylate, Chinese J. Polym. Sci., 23 (2005) 219–225.
[45] X.N. Wang, Q.Y. Yue, B.Y. Gao, X.H. Si, X. Sun, S.X. Zhang, Dispersion copolymerization of acrylamide and dimethyl diallyl ammonium chloride in ethanol-water solution, J. Appl. Polym. Sci., 120 (2011) 1496–1502.
[46] X.H. Peng, X.C. Peng, J.R. Shen, Water-soluble copolymers. III. Two-step terpolymerization of acrylamide, acrylic acid, and acryloyloxyethyltrimethyl ammonium chloride, J. Appl. Polym. Sci., 103 (2007) 3278–3284.
[47] Y. Liao, H.L. Zheng, Q. Li, Y.J. Sun, D. Li, W.W. Xue, UV-initiated polymerization of hydrophobically associating cationic polyacrylamide modified by a surface-active monomer: A comparative study of synthesis, characterization, and sludge dewatering performance, Ind. Eng. Chem. Res., 53 (2014) 11193–11203.
[48] M.L. Zhang, Q.F. Yao, W.J. Guan, C. Lu, J.M. Lin, Layered double hydroxide-supported carbon dots as an efficient heterogeneous Fenton-like catalyst for generation of hydroxyl radicals, J. Phys. Chem. C., 118 (2014) 10441–10447.
[49] S.J. Lu, R.X. Liu, X.M. Sun, A study on the synthesis and application of an inverse emulsion of amphoteric polyacrylamide as a retention aid in papermaking, J. Appl. Polym. Sci., 84 (2002) 343–350.
[50] M. Yang, M. Jonsson, Evaluation of the O2 and pH effects on probes for surface bound hydroxyl radicals, J. Phys. Chem. C., 118 (2014) 7971–7979.
[51] P.C. Selvaraj, V. Mahadevan, The decomposition of H_2O_2 catalyzed by polymer supported transition metal complexes, J. Molec. Catal. A. Chem., 120 (1997) 269–294.
[52] H.R. Lin, Solution polymerization of acrylamide using potassium persulfate as an initiator: Kinetic studies, temperature and pH dependence, Eur. Polym. J., 37 (2001) 1507–1510.
[53] X. Li, H.L. Zheng, B.Y. Gao, Y.J. Sun, X.M. Tang, B.C. Xu, Optimized preparation of micro-block CPAM by response surface methodology and evaluation of dewatering performance, RSC Adv., 7 (2017) 208–217.
[54] S.A. Seabrook, R.G. Gilbert, Photo-initiated polymerization of acrylamide in water, Polymer, 48 (2007) 4733–4741.
[55] C.W. Luo, J. Ma, J. Jiang, Y.Z. Liu, Y. Song, Y. Yang, Y.H. Guan, D.J. Wu, Simulation and comparative study on the oxidation kinetics of atrazine by UV/H_2O_2, UV/HS and UV/S_2, Water Res., 80 (2015) 99–108.
[56] M. Cheng, G.M. Zeng, D.L. Huang, C. Lai, P. Xu, C. Zhang, Y. Liu, Hydroxyl radicals based advanced oxidation processes (AOPs) for remediation of soils contaminated with organic compounds: A review, Chem. Eng. J., 284 (2016) 582–598.
[57] N.H. Ince, M.I. Stefan, J.R. Bolton, UV/H_2O_2 degradation and toxicity reduction of textile azo dyes: Remazol Black-B, a case study, J. Adv. Oxid. Technol., 2 (2017) 442–448.
[58] L. Besra, D.K. Sengupta, S.K. Roy, P. Ay, Influence of polymer adsorption and conformation on flocculation and dewatering of kaolin suspension, Sep. Purif. Technol., 37 (2004) 231–246.
[59] J.Y. Ma, K. Fu, X. Fu, Q.Q. Guan, L. Ding, J. Shi, G.Z. Zhu, X.X. Zhang, S.H. Zhang, L.Y. Jiang, Flocculation properties and kinetic investigation of polyacrylamide with different cationic monomer content for high turbid water purification, Sep. Purif. Technol., 182 (2017) 134–143.
[60] H.L. Zheng, Y.J. Sun, J.S. Guo, F.T. Li, W. Fan, Y. Liao, Q.Q. Guan, Characterization and evaluation of dewatering properties of PADB, a highly efficient cationic flocculant, Ind. Eng. Chem. Res., 53 (2014) 2572–2582.

[61] W. Brostow, S. Pal, R.P. Singh, A model of flocculation, Mater. Lett., 61 (2007) 4381–4384.
[62] P. Pal, J.P. Pandey, G. Sen, Modified PVP based hydrogel: Synthesis, characterization and application in selective abstraction of metal ions from water, Mater. Chem. Phys., 194 (2017) 261–273.
[63] D.J.A. Williams, R.H. Ottewill, The stability of silver iodide sols in the presence of polyacrylic acids of various molecular weights, Kolloid-Zeitschrift und Zeitschrift für Polymere, 243 (1971) 141–147.
[64] J.Y. Ma, K. Fu, L.Y. Jiang, L. Ding, Q.Q. Guan, S.H. Zhang, H.W. Zhang, J. Shi, X. Fu, Flocculation performance of cationic polyacrylamide with high cationic degree in humic acid synthetic water treatment and effect of kaolin particles, Sep. Purif. Technol., 181 (2017) 201–212.
[65] H. Kheradmand, J. Francois, V. Plazanet, Hydrolysis of polyacrylamide and acrylic acid-acrylamide copolymers at neutral pH and high temperature, Polymer., 29 (1988) 860–870.